THE RESPONSE OF A MODEL HEXAGONAL DETECTOR AREA TO RADIO SIGNALS FROM ULTRA-HIGH ENERGY COSMIC RAYS AIR SHOWERS

P. G. ISAR[1], D. HÎRNEA[1]

[1]Institute of Space Science (ISS), Măgurele-Bucharest, Romania
E-mails: *gina.isar@spacescience.ro, dragos.hirnea@spacescience.ro*

Compiled June 29, 2021

Ultra-high energy cosmic rays (UHECRs) are subatomic charged particles accelerated at astounding energies in violent astrophysical processes. They travel vast distances through the outer space and every so often enter the Earth's atmosphere. Here they interact and initialize the development of cascading secondary elementary particles, known as extensive air showers (EASs). From characteristics of the induced air showers, properties of primary cosmic rays are deduced, such as mass, energy and arrival direction, and so they serve in complementary indirect measurements of UHECRs. The radio detection technique is used to record radio signals emitted by the electromagnetic component of air showers, employing arrays of radio antennas.

In this paper we look at the response of a model hexagonal layout of 37 antennas, by using a sample of CoREAS simulated proton events at two different energies: 10^{18} and 10^{19} eV. First we look at the general characteristics of the registered polarized radio signals, in correlation with the position of the observer, with respect to the shower core and distance to the showers axis. In a second step we explore some particular characteristics of the radio emission.

Key words: cosmic rays, air showers, radio detection, Monte Carlo simulations.

1. INTRODUCTION

Ultra High Energy Cosmic Rays which exceed energies above 10^{18} eV are the most energetic particles measured on Earth. Their sources remain unknown, having a low flux from approximately one particle/square kilometer/year to one particle/square kilometer/century at highest energies of about 10^{20} eV. Therefore, UHECRs are measured indirectly on Earth, through the detection of extensive air showers developed in the Earth's atmosphere.

Various detection techniques are being used widely so far in the observation of cosmic rays induced air showers, such as surface particle detectors, underground muon counters, fluorescence telescopes, radio detectors. In this paper we will refer to the radio detection technique, which is been successfully utilised in various experiments [1] for the reconstruction of primary cosmic ray's energy, mass and arrival direction. Moreover, the radio detection method is very promising for measurements of inclined air showers at large scales [2].

The radio detection technique relies on the radio emission mechanisms which occur during the air shower development. The emitted radio signals are dominantly generated by the geomagnetic effect, in which the secondary charged particles (electrons and positrons) developed in the showers are deviated in the Earth's magnetic field. A secondary radio emission contribution arises from the Askaryan effect, which is due to variation in time of the negative charge excess generated in the shower front. Nevertheless, contributions from each emission mechanism may vary with the incoming shower direction, respective with the azimuth angle, with respect to the geomagnetic filed at the experiment location.

In the following we look at the radio emission characteristics and the detector response, using a sample of events simulated for a model-like hexagonal layout array of radio stations, with application at the Auger Engineering Radio Array [3].

2. MONTE CARLO SIMULATIONS

This work is based on CoREAS (Corsika-based Radio Emission from Air Showers) Monte Carlo simulations [4], part of CORSIKA (COsmic Ray SImulations for KAscade) [5], which implements the end point formalism for calculation of the radio emission from air showers. Within CoREAS, the radio signals are fully simulated in an infinite bandwidth of frequencies, therefore we used the REASPlot tool [6] to filter the raw data in the 30 - 80 MHz range, which corresponds to the frequency band of the radio antennas used at the Pierre Auger Observatory [7].

A sample of events were simulated for proton, as primary cosmic ray particle, at two primary energies, 10^{18} eV and respectively 10^{19} eV, for a hexagonal grid of 37 radio stations (A37). The hexagonal-model detector area has 375 m spacing between antennas, spread over 1 km^2 at an altitude of about 1450 m, representative to the Pierre Auger Observatory. The sample of events comprise a number of 64 showers, with geometries structured into eight zenith angles (from 10 to 80 degrees, in steps of 10) and eight azimuth angles (from 0 to 315 degrees, in steps of 45).

We also refer to the Auger geometry convention, where the East arrival direction of showers is defined by the 0^o azimuth angle and the North direction by 90^o, in counter clockwise. While the CORSIKA geometry convention describes the showers arriving from East with an azimuth angle of 90^o and the showers arriving from North with an azimuth angle of 180^o, also in counter clockwise, the geometries of the simulated showers were transformed accordingly to the Auger convention. The same coordinate system is applied for the Earth's magnetic field at the Auger location, of which components are: $\theta_B = 53.4^o$ (zenith) and $\phi_B = 87.3^o$ (azimuth).

3. RESULTS

In the following we describe some main results of the analysis, starting first with general characteristics of the simulated radio emission and the detector response. A second view will be addressed to some particular details of the simulated polarised radio signals for proton induced air showers at two primary energies.

3.1. GENERAL CHARACTERISTICS

In Figure 1 is shown a graphical representation of the electric field strength as function of the distance from each antenna to the shower axis. One can observe an amplitude decrease with distance and energy, showing however a flattening in the lateral distribution for higher zenith angles, moreover for values above 70 degrees.

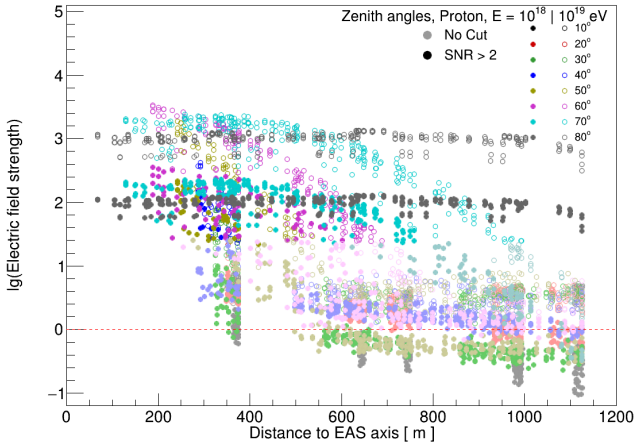

Fig. 1 – Lateral distribution of the electric field strength, with the color code on zenith angle, with/-out SNR cut.

The same is seen on the time-amplitude maps in Figure 2, were patterns of a vertical and an inclined shower are shown. The higher the zenith angle the larger the number of antennas with high signals recorded, in comparison with the lower the zenith angle the less number of antennas with high signal recorded.

The time response of each antenna from the A37 model-like array is highlighted by the color of the marker and the recorded amplitude by the size of marker. For each simulated shower the response time of antennas is calculated by CoREAS relative to the exact moment when the first secondary particle reaches the shower core; a fast response is described by negative values and a delayed response by positive values. For vertical showers (Figure 2a), the radio signal rapidly decrease with

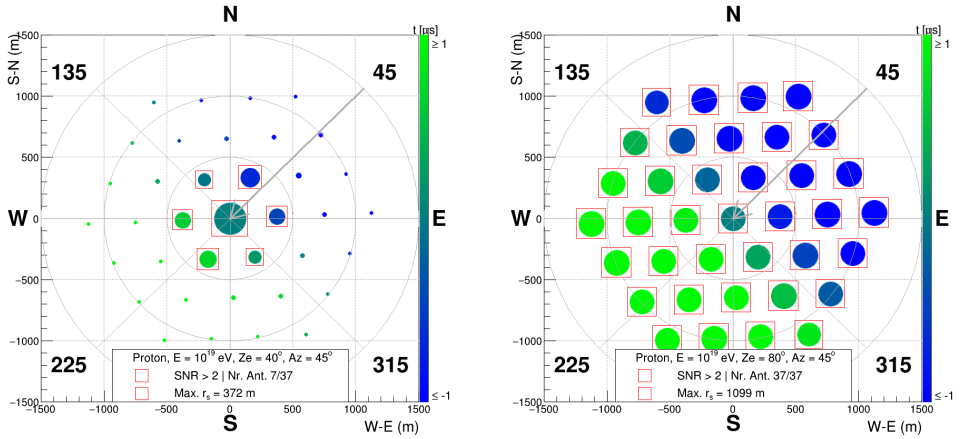

(a)Vertical EAS (b)Inclined EAS

Fig. 2 – Maps of the recorded simulated radio signals for two different shower geometries, highlighting the response of the antennas with SNR above two in open red square markers.

the lateral distance to the shower axis, and only a small number of antennas around the shower core (placed at the center of the array), also highlighted with red squares, record high signals to noise ratio (SNR) above two. By contrast, the radio emission of inclined showers (Figure 2b) covers a larger detection area and a higher number of antennas record high signals accordingly.

Figure 3 shows a clear representation of the differences between vertical and inclined showers, as seen from the A37 array response. It can be observed how the number of antennas with high SNR values increases with zenith angle and energy of the primary particle (top panel). However, the differences between the two displayed energies are minimal at the zenith angle of 80^o, indicating that for showers with high zenith angles and high primary energy, the recorded signals with high SNR cover a larger area than the one covered by A37. The same is observed at the correlation between the medium antenna distance to the shower axis as function of zenith angle (bottom panel), with the color code on azimuth angle, for signals which pass the SNR cut above two. The medium antenna distance grows with zenith angle at both energies, moreover showing higher values at 10^{19} eV for showers coming from the South, except for the zenith angle of 80^o where variations are minimal.

3.2. DETECTOR RESPONSE

The A37 radio array used in the present analysis features seven rows of antennas positioned along the East - West axis, placed at equal distances towards the North - South axis, with respect to the shower core fixed in the center of the array (as seen in

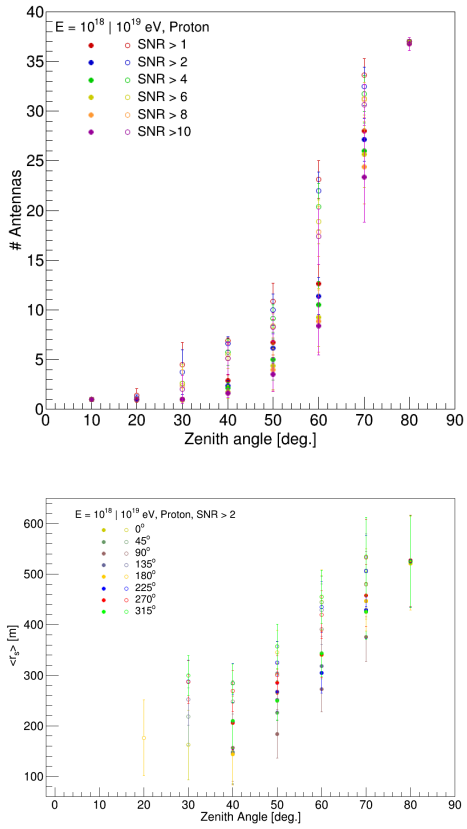

Fig. 3 – Representation of antenna number, with the color code on SNR, as function of zenith angle for proton at two energies (top), as well as medium distance to the shower axis, with the color code on azimuth angle and SNR above two (bottom). The error bars represent the mean signal per zenith bin.

Figure 2). In Figure 4 is shown the detector response, defined by the seven antenna selections with different markers, with the color code on the shower zenith angle, for the primary energy of 10^{19} eV, SNR above two and showers coming from four directions: North, South, East and West. The marker type indicates the following antenna selection: C (antennas along the central axis); N1, N2, N3 (antennas positioned towards North); S1, S2, S3 (antennas positioned towards South); the higher the number of the antenna selection the greater the distance to the shower core, i.e. N3 represents the farther distant antennas towards North, and S3 the farther distance antennas towards South. The radio signals registered from vertical showers show a narrow distribution close to the shower axis and the shower core, while contrarily, the inclined showers show a much wider lateral distribution of the signal, which becomes flattening across the entire radio array for higher zenith angles, moreover for

80^o. In particular, the number of stations with high signals is increasing with primary energy and zenith angle, as it is also shown in Figure 3. Similar features are highlighted with the color code on the azimuth angle, in particular showing higher signals for showers coming from the South, as expected, due the geomagnetic angle at the Pierre Auger experiment location. This is a clear evidence, however, that for recording highly inclined events a larger detection area is needed, in contrast with a small one, with low distance spacing between antennas, suitable for vertical events.

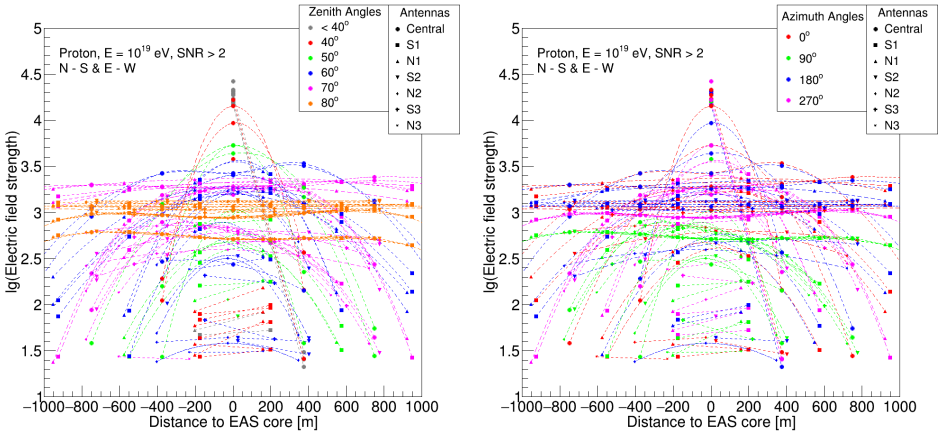

Fig. 4 – The detector response of A37 with seven antenna selections (upwards and downwards to the central horizontal aligned antennas along the East and West directions) for four arrival directions of air showers (North, South, East, West), as function of zenith -left and azimuth -right.

3.3. RADIO EMISSION COMPONENTS

The radio emission of cosmic rays induced air showers is the result of a superposition between two components, the geomagnetic and the Askaryan. They both are treated fully in the CoREAS Monte Carlo simulations, while the $\vec{v} \times \vec{B}$ Lorentz force model describes the geomagnetic component only [8, 9]. Having these two methods applied to our sample of events, one can differentiate between the radio emission mechanisms, by using a ratio between the simulated and modeled signals, for each polarization component (North-South and East-West).

In Figure 5 is shown a good correlation between Monte Carlo simulations and the $\vec{v} \times \vec{B}$ model, which is indicated by the diagonal distribution, for two primary particle energies and SNR above two. Nevertheless, for showers propagating from the North and South directions, as highlighted in red, it can be seen a lateral deviation from the diagonal, which is associated with the Askaryan component of the radio emission, treated in simulations only, and thus showing additional contribution to the

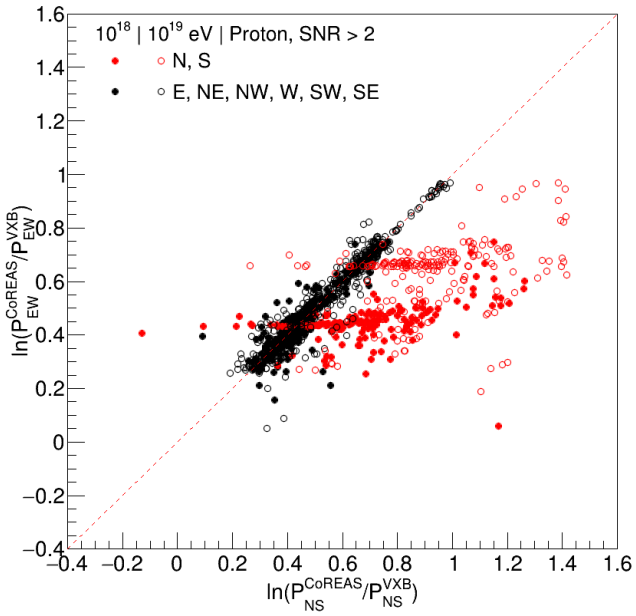

Fig. 5 – The simulated electric field strength in report to the $\vec{v} \times \vec{B}$ model, for each EW and NS polarization component of the signal.

dominant geomagnetic component.

3.4. POLARIZATION CHARACTERISTICS

The geomagnetic and Askaryan components of the radio emission of air showers feature different polarization characteristics as a result of their corresponding emission mechanisms. Because the geomagnetic emission is caused by the separation of the positive and negative charged particles in the shower under the action of the Lorentz force induced by the Earth's magnetic field, the electric field generated is linearly polarised in the direction of the Lorentz force [8]. The Askaryan emission, produced by the negative charge excess in the shower front, shapes radially polarized signals in the direction of the shower axis.

In Figure 6 we look at the polarization patterns of the radio signals recorded in the North-South and East-West antenna channels by using a selection of antennas positioned symmetric to the North and South directions, with respect to the shower core fixed in the center of the array. It can be observed a difference between a vertical event (Figure 6a), where signals show more like radial polarization and an inclined event (Figure 6b), which shows linear polarization. At the same time for the vertical event it can be observed a difference between the polarization axis in the NS-EW

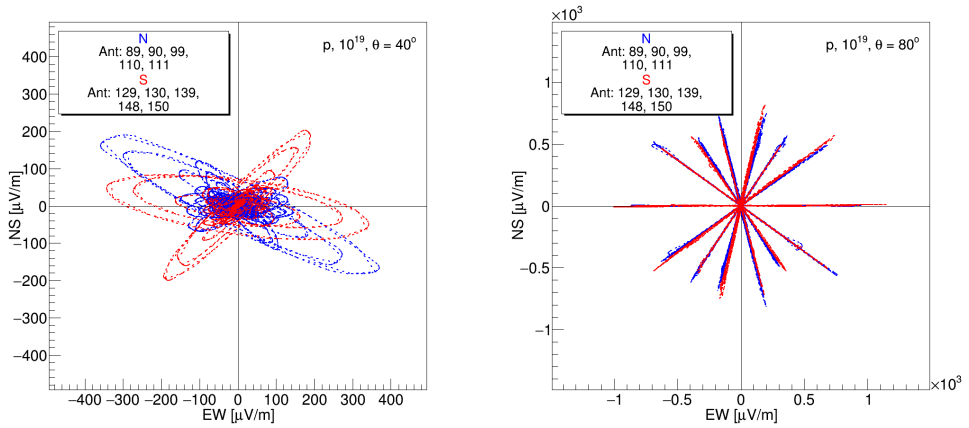

(a) Circular polarization (b) Linear polarization

Fig. 6 – Polarized radio signals showing different polarization patterns for vertical (left) and inclined events (right).

frame for the antennas positioned to the North and South from the shower core. This indicates a variation of the radio signal, with respect of the observer's distance to the shower axis, which increases with zenith angle (as also shown in Figures 1, 2).

3.5. POLARIZATION ASYMMETRY

We also looked at the North-South and East-West polarisation asymmetries, as measured by the A37 model detector area. The asymmetry percentage is calculated individually per simulated event, independent for each polarization channel (eqs. 1),

$$a_{NS}[\%] = \frac{2\cdot(A_S - A_N)}{A_S + A_N}; a_{EW}[\%] = \frac{2\cdot(A_W - A_E)}{A_W + A_E}. \quad (1)$$

where A_S and A_N are sums over the NS polarization amplitudes recorded by the antennas positioned in the North and South directions, with respect to the shower core; similarly, A_W and A_E are sums over the EW polarization amplitudes recorded by the antennas positioned in East and West directions.

Figure 7 shows the results obtained with two methods, in comparison for two primary energies and SNR above two; one method was applied to filtered data recorded by all antennas, except the central antenna with ID 120 (left panel), and a second method was applied to a selected list of antennas positioned in a symmetric grid relative to the shower core, on the NS and EW directions. After calculating each polarization asymmetry in percentage for individual simulations, a mean value (the

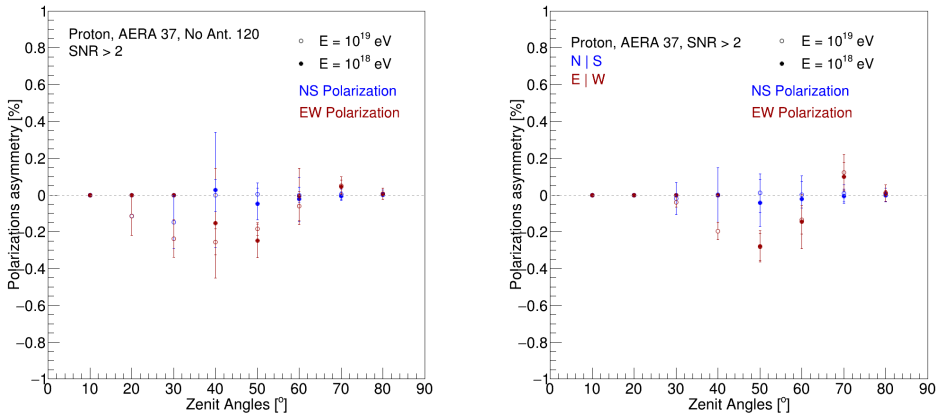

(a)Without central antenna. (b)A selection of antennas

Fig. 7 – Polarization asymmetry with the color code on the NS and EW directions as function of zenith angle, for two primary energies corresponding to proton and with SNR above two.

error bars) is obtained per zenith angle for all eight corresponding azimuth angles. It can be observed a stronger asymmetry in the EW polarization, moreover at lower zenith angles and for a higher primary energy. The polarization asymmetry decreases with increasing the zenith angle, which becomes negligible at zenith of 80^o.

4. CONCLUSIONS

The present work it aimed to analyse the detector response of a model-like hexagonal radio array for radio emission simulations of a sample of air showers at two primary energies, initiated by a proton as primary particle with various propagating geometries. The obtained results showed a clear improvement of the detector response with an increased shower zenith angle and primary particle energy. In particular, from analysis of the radio signals recorded by the model detector area - A37, for Monte Carlo simulations in comparison with a simplified model, the dominant presence of the geomagnetic component of the radio emission is being highlighted, showing an additional contribution from the Askaryan component present in simulations only, moreover for showers coming from the North and South directions. This seems to be correlated with the particular characteristics of the air showers radio emission at the Pierre Auger Observatory, due to the direction towards North of the geomagnetic field at the experiment location. The increased inclination degree of the incoming showers is also an important factor for contribution of the radio emitted signals at large distances from the shower core. This will have a direct impact to

the radio polarization measurements at large scale arrays, which is the aim of further studies with application to the present upgrade of the Pierre Auger Observatory.

This analysis, among others, is implemented into an YAD (yet another dialog) tool [11] for creating graphical dialogs from shell scripts based on the user interface GTK+ and programming languages like Unix Shell and C. The developed YAD user interface [12] is programmed to use ROOT (data analysis framework) [13] scripts, written in C/C++, through which the data analysis is made and various graphics are produced and displayed automatically in the interface. This tool is aimed for new users, with application on educational purposes as well, for an easy and friendly introduction to the physics of the present studies.

Acknowledgements. This work was supported by a grant of the Romanian National Authority for Scientific Research and Innovation, CNCS/CCCDI - UEFISCDI, project number PN-III-P1-1.2-PCCDI-2018-0839, within PNCDI III, as well as by PN19150201/16N/2019.

REFERENCES

1. Frank G. Schroeder, "*Radio detection of cosmic-ray air showers and high-energy neutrinos*", Progress in Particle and Nucl. Phys., 93 (1-68) 2017
2. Aab, A. ... Isar P.G. et al. Pierre Auger Coll., "*Observation of inclined EeV air showers with the radio detector of the Pierre Auger Observatory*", JCAP 10 (2018) 026
3. Aab, A. ... Isar P.G. et al. Pierre Auger Coll., "*Energy estimation of cosmic rays with the Engineering Radio Array of the Pierre Auger Observatory*", Phys. Rev. D 93 (122005) 2016
4. Huege, T., "*CoREAS 1.4 User's Manual*", 2019: https://web.ikp.kit.edu/huege/downloads/coreas-manual.pdf
5. Heck, D., Knapp, J., Capdevielle, J. N., Schatz, G., and Thouw, T., "*CORSIKA: a Monte Carlo code to simulate extensive air showers*", 1998.
6. Huege, T., "*REAS 3.1 User's Manual*", 2011: http://citeseerx.ist.psu.edu/viewdoc/download?doi=10.1.1.574.3995&rep=rep1&type=pdf
7. Abreu, P. et al. Pierre Auger Coll., "*Antennas for the detection of radio emission pulses from cosmic-ray induced air showers at the Pierre Auger Observatory*", Journal of Instrumentation, 7(10):P10011–P10011, 2012
8. Isar, P. G., Apel, W. D., Arteaga, J. C., et al. the LOPES Coll.,"*Radio emission of energetic cosmicray air showers: Polarization measurements with LOPES*", NIMA 604 (2009) S81
9. Isar, P. G., Hirnea, D., and Jipa, A., "*Cosmic rays air showers properties and characteristics of the emitted radio signals using analytical approaches and full Monte Carlo simulations*", Rom. Rep. Phys., 72(1):301, 2020
10. Huege, T. for Pierre Auger Coll., "*Probing the radio emission from cosmic-ray-induced air showers by polarization measurements*", ICRC 2013
11. The YAD website: https://sourceforge.net/projects/yad-dialog/
12. A short presentation of the YAD developed tool is available at the following website: https://www.spacescience.ro/collaborations/auger/
13. ROOT (analyzing petabytes of data, scientifically), an open-source data analysis framework used by high energy physics and others. https://root.cern/